

# Factors Leading to Extreme Precipitation on Dominica from Tropical Storm Erika (2015)

ALISON D. NUGENT

*University of Hawai'i at Mānoa, Honolulu, Hawaii*

ROSIMAR RIOS-BERRIOS<sup>a</sup>

*University at Albany, State University of New York, Albany, New York*

(Manuscript received 21 August 2017, in final form 1 December 2017)

## ABSTRACT

Tropical cyclones are generally characterized by strong rotating winds, and yet, the associated rainfall can be equally destructive. Tropical Storm Erika (2015) is an example of such a cyclone whose heavy rainfall south of the storm center was responsible for significant loss of life and property. Tropical Storm Erika was a weak tropical storm in a sheared environment that passed through the Lesser Antilles on 27 August 2015. Radar and rain gauges measured at least a half meter of rainfall on the Commonwealth of Dominica in about 5 h. In this study, an analysis of several observational datasets showed that the combination of a sheared environment, dry northern sector, and mesovortex contributed to the significant storm precipitation. The sheared environment affected the storm structure, causing it to weaken, but also organized convection and precipitation in the region that passed over Dominica. Furthermore, a mesovortex embedded within the storm persisted over Dominica, leading to enhanced rainfall totals. Understanding the factors leading to heavy rainfall for this case is important for future prediction of similar weak, sheared tropical storms passing near mountainous islands.

## 1. Introduction

The tropical storm (TS) stage of tropical cyclones is the least studied stage, in part because higher-category storms are considered to hold the greatest threat to society (Dolling and Barnes 2012). While it is true that strong tropical cyclones have faster wind speeds and higher rainfall rates (Lonfat et al. 2004), the heavy precipitation accompanying tropical storms can also pose a substantial threat to society. Indeed, heavy precipitation is the second-leading cause of fatalities associated with tropical cyclones over the United States, second only to storm surge (Rappaport 2014). An understanding of factors leading to and enhancing heavy precipitation associated with tropical storms is of utmost importance for accurate prediction of tropical cyclone-related impacts.

Tropical Storm Erika (2015) is an example of a storm with relatively weak winds but heavy precipitation that

caused significant damage and loss of life on the Commonwealth of Dominica (hereinafter Dominica). Part of the reason the impacts of TS Erika were so great on Dominica was due to the common presumption that tropical storms with weaker winds are less dangerous than hurricanes (M. Alexander 2016, personal correspondence). Understanding the environment that TS Erika developed in, as well as the storm structure, will help to properly predict future similar events.

TS Erika formed in the Atlantic Ocean approximately 900 nautical miles (n mi; 1 n mi = 1.852 km) east of the Lesser Antilles (Pasch and Penny 2016). During its early stages, TS Erika was forecast to strengthen to a category 1 hurricane on its westward track and curve northward toward Miami, Florida. Instead, its surface center of circulation passed over the northern coast of Guadeloupe on 27 August 2015 near the peak of its intensity [1001 mb (1 mb = 1 hPa) and 45 kt (1 kt = 0.5144 m s<sup>-1</sup>)], decaying a day later to a low-pressure disturbance before crossing the Dominican Republic. See Fig. 1 for the best track map of TS Erika's path.

As the center of TS Erika crossed Guadeloupe, Dominica (just to the south of Guadeloupe) received

<sup>a</sup> Current affiliation: National Center for Atmospheric Research, Boulder, Colorado.

Corresponding author: Alison D. Nugent, anugent@hawaii.edu

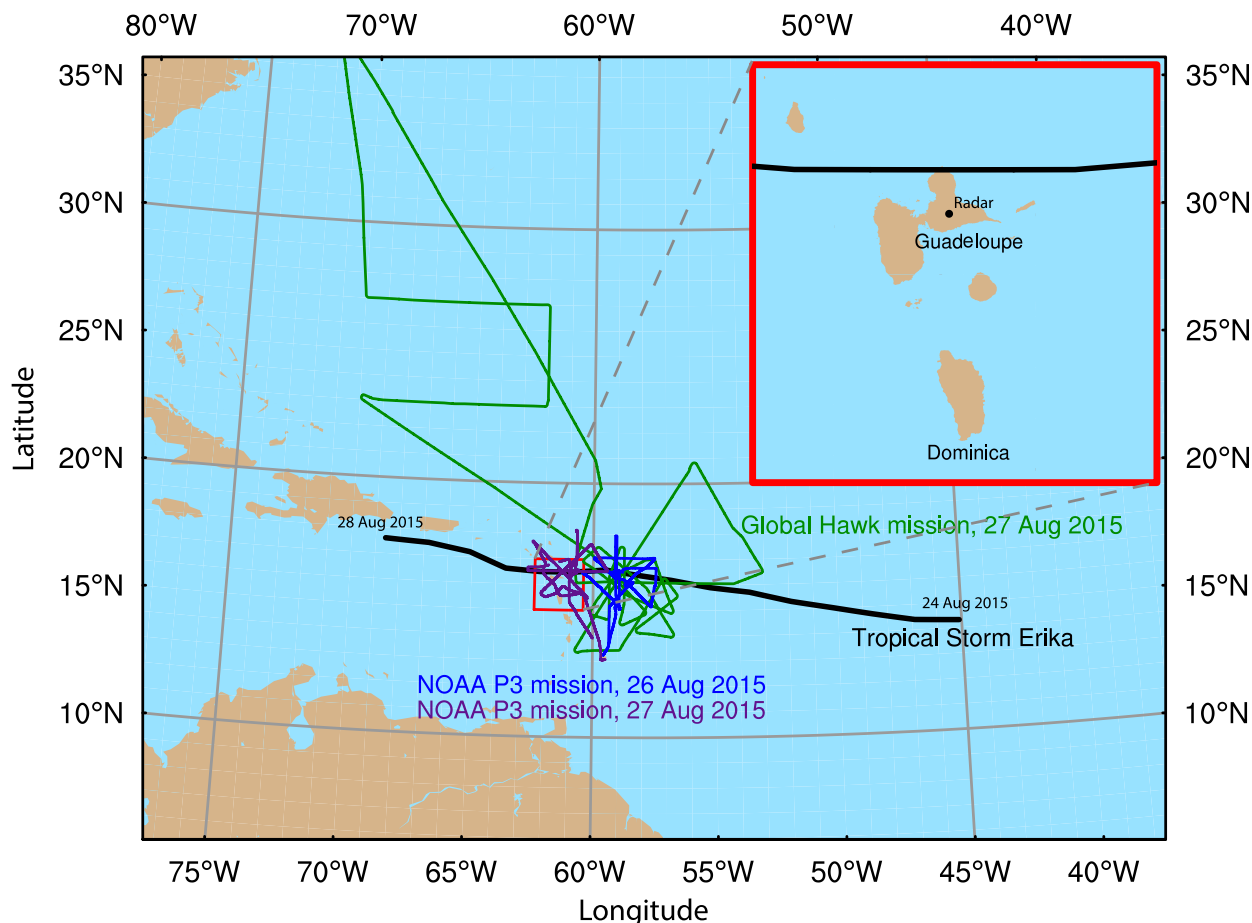


FIG. 1. A map showing best track estimates of TS Erika's position as it crossed from the Atlantic Ocean into the Caribbean Sea from 24 Aug to 28 Aug 2015. Also shown are the flight tracks of two NOAA P-3 missions and a Global Hawk mission during SHOUT. The inset shows a close-up of TS Erika's path by Guadeloupe and the location of the Guadeloupe Météo-France radar.

torrential rain and was severely impacted by flooding and mudslides. The rainfall resulted in peak flood flows that lie on the global maximum flood peak envelope as a function of watershed area (Ogden 2016). TS Erika's impacts on Dominica included the following: 30 direct deaths, 574 people left homeless, and 271 houses damaged or destroyed (Pasch and Penny 2016). Serious damage was also reported to roads, bridges, buildings, and other infrastructure. After the event, the prime minister of Dominica, Roosevelt Skerrit, said in a televised address that TS Erika "set [Dominica] back by 20 years." The name "Erika" has since been retired because of this event, primarily due to the destruction it caused on Dominica. TS Erika is only the second tropical system to have its name retired without reaching hurricane strength.

The impacts of precipitation from TS Erika on Dominica expose a limitation of current scientific knowledge: What factors contribute to extreme precipitation totals during the passage of weak tropical cyclones near land? To address this issue, a number of observational datasets of TS Erika's

passage over Dominica are used to explore factors contributing to the devastating precipitation totals on Dominica. Section 2 contains a description of the observational platforms. Precipitation observations are in section 3, an overview of results and the structure of TS Erika are in section 4, and, finally, a discussion and conclusions are in section 5.

## 2. Observational datasets

Aircraft observations of TS Erika were collected to aid in forecasting the event. In addition, longer-term ground sites already in place in the Caribbean observed the passage of TS Erika. The observational datasets are described below.

### a. Airborne observations

Two types of aircraft missions were flown into and around TS Erika. The first type consisted of research missions coordinated between the National Oceanic and Atmospheric Administration (NOAA) Aircraft Operations Center (AOC) and Hurricane Research Division (HRD).

Together, NOAA AOC and HRD programs flew several research and synoptic surveillance missions with the NOAA P-3 and Gulfstream IV aircrafts. Observations from two research missions with the NOAA P-3 were considered here: 1) a mission spanning 1706–2316 UTC 26 August 2015 and 2) a mission spanning 0456–1146 UTC 27 August 2015. The tracks of those two flights are shown in Fig. 1. The second type of aircraft mission was a research flight with NASA's Global Hawk aircraft during the NOAA Sensing Hazards with Operational Unmanned Technology (SHOUT) project, funded by the NOAA Unmanned Aircraft Systems program. The SHOUT mission's goal was to obtain observations over the ocean, specifically targeted on weather events that needed model forecast improvements. Two SHOUT missions were flown around TS Erika, but here, the focus will be on the mission spanning 1400 UTC 26 August to 1043 UTC 27 August 2015 (Fig. 1). Specific instruments used during these missions are described below.

#### 1) TAIL DOPPLER RADAR

On board the NOAA P-3 aircraft was a tail Doppler radar (TDR). The TDR has a 3.22-cm wavelength and 9315-MHz frequency, and it can perform range–height scans from the tail of the aircraft (e.g., Jorgensen et al. 1983; Susca-Lopata et al. 2015). At 3.22-cm wavelength, the TDR is an X-band radar, which makes it susceptible to attenuation in heavy rain. However, the Doppler capabilities of the radar make it especially useful for remote observation of wind characteristics in a tropical storm (Lorsolo et al. 2010).

#### 2) HIGH-ALTITUDE MONOLITHIC MICROWAVE INTEGRATED CIRCUIT SOUNDING RADIOMETER

On board the Global Hawk was a High-Altitude Monolithic Microwave Integrated Circuit (MMIC) Sounding Radiometer (HAMSR). The HAMSR operated with 25 spectral channels in three bands (50–60, 118, and 183 GHz), and from its measurements, one can infer the 3D distribution of temperature, water vapor, and cloud liquid water in the atmosphere (Brown et al. 2011). This instrument scans within a range of  $\pm 60^\circ$  across the flight track, but only the range of  $\pm 45^\circ$  across track was considered here because of large errors outside that range (Brown et al. 2011).

#### 3) DROPWINDSONDES

Also on board the Global Hawk was a dropwindsonde system known as the Advanced Vertical Atmospheric Profiling System (AVAPS). The dropwindsondes collect measurements of temperature, pressure, relative humidity, wind speed, and direction in the atmosphere (Hock and Franklin 1999). Dropwindsondes used during the SHOUT field campaign recorded measurements

every 0.25 s from the flight level [approximately 60 000–65 000 ft (18 288–19 812 m)] to the surface.

### b. Ground observations

#### 1) RAIN GAUGES

A series of 10 rain gauges were stationed across the high terrain of Dominica. Seven gauges were operational during the storm passage, and their locations are shown in Fig. 2a. The rain gauges were HOBO tipping-bucket gauges that recorded at a resolution of 0.2 mm to the nearest second (<http://www.onsetcomp.com/products/data-loggers/rg3>). All rain gauges were located in the southern portion of the island. For more information on the rain gauges installed on Dominica, see Smith et al. (2009a, their Fig. 1 and Table 1).

#### 2) RADAR

In addition to the rain gauge measurements, a Météo-France S-band radar on Guadeloupe recorded the precipitation from TS Erika in 5-min plan position indicator (PPI) scans (location shown in Fig. 1). The processing method for storm-accumulated precipitation is described in Ogden (2016). In addition to precipitation measurements from the radar, a storm-tracking algorithm was used to investigate the movement of reflectivity cells within the radar domain. This algorithm is called Thunderstorm Identification, Tracking, Analysis, and Nowcasting (TITAN; Dixon and Wiener 1993). The method used subsequent scans of radar reflectivity to match convective features using an optimization algorithm. The result is a motion vector showing where the feature moved from one frame to the next, and from that vector, velocity can be inferred based on the distance moved and the time between the two radar scans. In the case of the Météo-France Guadeloupe radar, the radar scans were 5 min apart, allowing easy tracking and reasonable temporal resolution velocity information.

Observational datasets from the various aircraft platforms (aircraft Doppler radar, radiometer, and dropwindsondes) and ground platforms (rain gauges and radar) are combined to get a full understanding of precipitation and the dynamical aspects of TS Erika before, during, and after its passage near Dominica.

### 3. Precipitation

TS Erika formed at approximately  $45^\circ\text{W}$  and traveled primarily westward until it decayed, just before it reached  $70^\circ\text{W}$ , from 1800 UTC 24 August to 1800 UTC 28 August 2015 (Fig. 1). The primary low-pressure center of TS Erika passed approximately 100 km to the north of Dominica, directly over the northern portion of Guadeloupe (see inset in Fig. 1). The convective region of TS Erika passed over Dominica following the passage

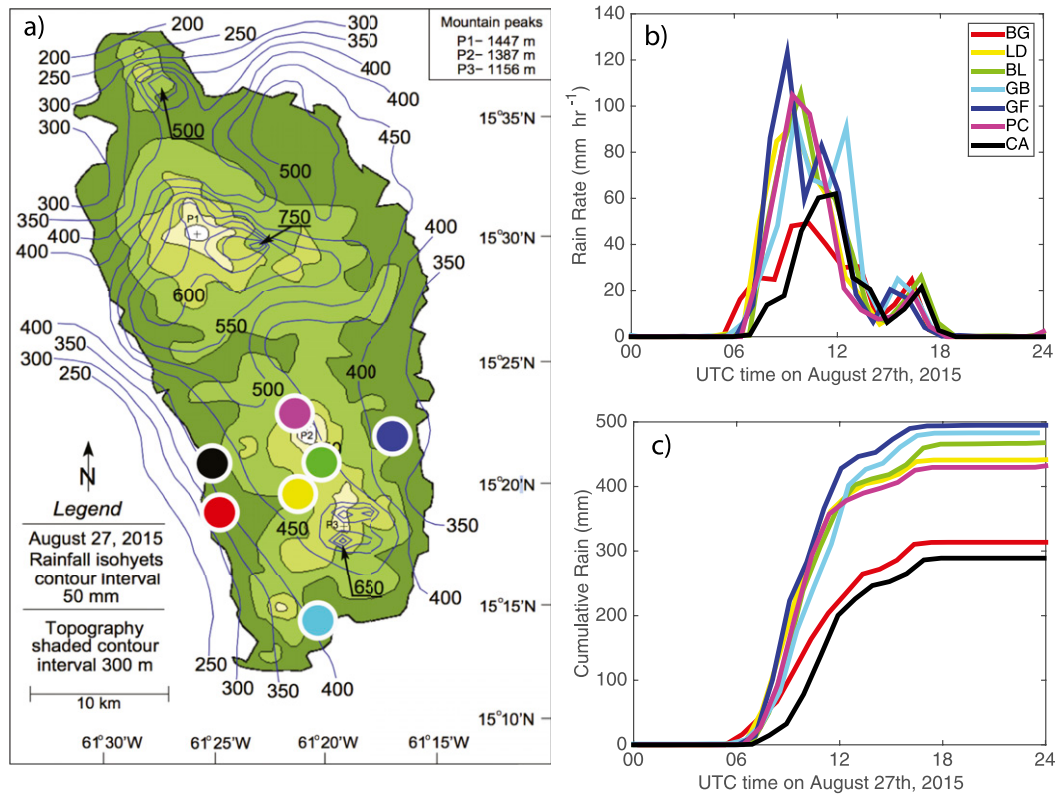


FIG. 2. (a) A map of Dominica showing terrain height in shaded color contours in 300-m intervals and storm precipitation total isohyets from 27 Aug 2015 in 50-mm intervals, estimated by the Guadeloupe radar and calibrated to rain gauge ground observations. Rain gauge locations are given by the colored dots. [Image reproduced from Ogden (2016).] Also shown are (b) hourly rain rate ( $\text{mm h}^{-1}$ ) and (c) cumulative precipitation (mm) from the rain gauges on 27 Aug 2015.

of the low-pressure center. The passage of the convective region was well documented through ground-based precipitation measurements from radar and rain gauges.

Figure 2 shows TS Erika's precipitation on Dominica from two sources: the Météo-France Guadeloupe radar and a set of seven rain gauges on Dominica. The contours on the map in Fig. 2a show radar-derived precipitation with cumulative daily values for 24 h on 27 August 2015. In some places, cumulative amounts exceeded 500 mm, especially over high terrain. The radar values in Fig. 2a were calibrated with the rain gauges [for details on peak runoffs, see Ogden (2016), from which Fig. 2a was adapted]. Some pixels from the radar at low elevation angles have ground clutter or beam-blocking issues from the high terrain, described in Smith et al. (2009a). While this has been accounted for, some artifacts may remain.

Figures 2b and 2c show time series of rain rate and cumulative precipitation from the rain gauges, whose locations are shown on the map in Fig. 2a. A majority of the precipitation fell from 0600 to 1200 UTC, very early in the morning local time [Dominica local time is

Atlantic standard time (AST), or UTC - 4]. Precipitation on Dominica from TS Erika is also shown in Fig. 3. The colors in Fig. 3 show estimates of 1-hourly accumulated precipitation. It is useful to compare precipitation on Dominica through time between the radar and rain gauge records for additional clarity. The radar shows that early precipitation from TS Erika was focused in the south (Figs. 3b-d), but soon spread northward at later times (Figs. 3f-j). All rain gauges in the south had large precipitation accumulations, from 300 to 500 mm in about 5 h (Fig. 2b). The excellent agreement among rain gauges gives high confidence in the rain gauge results, and the excellent agreement between the timing of precipitation recorded with the radar and rain gauges gives high confidence in our knowledge of the temporal and spatial evolution of precipitation over Dominica.

The primary precipitation period from 0600 to 1200 UTC was followed by a much smaller, secondary maximum centered at 1600 UTC (Fig. 2b). This secondary maximum occurred after TS Erika passed over Guadeloupe, when southerly flow associated with the eastern

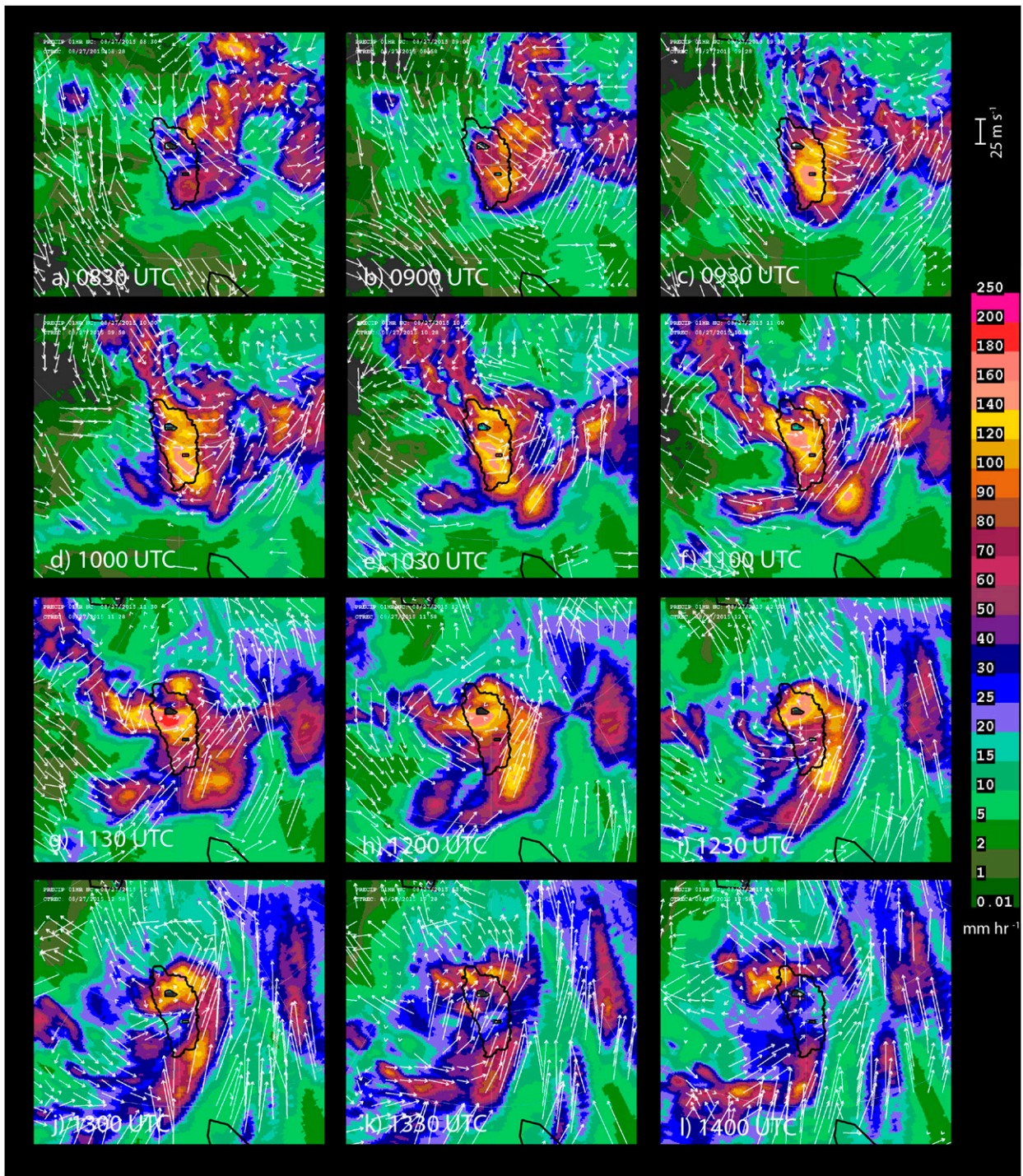


FIG. 3. Radar images from the Météo-France radar on Guadeloupe, whose location is shown in Fig. 1's inset. Direction and speed (scale in top right) of tracked features between subsequent frames (white vectors) and estimates of 1-hourly precipitation accumulation (colors, mm h<sup>-1</sup>) are shown. (a)–(l) Times are half-hourly, from top left to bottom right, covering 0830–1400 UTC 27 Aug 2015. The outline of Dominica (black) is centered in each image, and two beam-blocked regions are outlined (also in black). Note that the focus here is on tracked features and that precipitation accumulations have not been calibrated against the rain gauges, so they should only be used as a qualitative reference.

half of the storm dominated over Dominica (not shown). Dominica typically experiences trade wind flow from the east-northeast, but the passage of TS Erika to the north caused a substantial shift in the wind direction. Such a shift, combined with high humidity values at low latitudes, led to favorable conditions for continued precipitation over Dominica. While this does not appear to be the primary cause of the strong precipitation, it did bring additional showers after the passage of TS Erika.

The rain gauges with the least rain were the two low-elevation, west coast rain gauges [Botanical Gardens (BG) 18 m; Canefield Airport (CA) 10 m], but from Fig. 2a, it is clear the west coast rainfall gradients were strong (also seen in Figs. 3a–g). The high-altitude gauges [Laudat (LD) 592 m; Boeri Lake (BL) 861 m; Pond Casse (PC) 568 m], as well as the east and south coast gauges [Grand Fond (GF) 275 m; Grand Bay (GB) 525 m], all had surprisingly similar rain gauge–derived cumulative rain amounts and rain rates throughout the event, even though their elevations varied from 275 to 861 m, and their locations spanned the entire southern part of Dominica.

The heavy rainfall received by Dominica was a surprise: 3–5 in. of precipitation, with a maximum of 8 in. total accumulation, was the amount mentioned in all advisories for affected Caribbean islands by the National Hurricane Center prior to 1500 UTC 27 August 2015. In the 1500 UTC 27 August 2015 advisory, the maximum precipitation amount was increased to 12 in., after Dominica had already received 9 in. A look at the Global Forecast System (GFS) and European Centre for Medium-Range Weather Forecasts (ECMWF) global model (0.5° grid spacing) ensemble forecasts for 72- to 24-h lead times before the event show that none of the ensemble members at any time came close to predicting heavy precipitation on Dominica (not shown). The highest 24-h precipitation accumulation predicted for 27 August 2015 from one GFS ensemble member was just under 160 mm of precipitation, while the GFS and ECMWF ensemble averages were only 48 and 55 mm, respectively. The inability of global models to capture heavy precipitation on Dominica from TS Erika will be further discussed in section 5.

Heavy rainfall on Dominica is typical and expected climatologically, with an average of about 5  $\text{m yr}^{-1}$  of precipitation on the high terrain and a most frequent rain rate of 40  $\text{mm h}^{-1}$  (Smith et al. 2009a). Still, the precipitation received during TS Erika was unusually heavy. Orographic precipitation has been well studied on Dominica by a field campaign in 2011 (Smith et al. 2012) and a number of related studies (Smith et al. 2003, 2009a; Minder et al. 2013; Nugent et al. 2014). Based on prior knowledge of precipitation on Dominica, orographic enhancement due to forced mechanical lifting was hypothesized to be the primary reason for enhanced

precipitation during TS Erika. In everyday trade wind flow, the steep terrain of Dominica (Fig. 2a) causes additional vertical lifting and, thus, orographic enhancement of precipitation. Furthermore, clear orographic enhancement was found during Hurricane Dean, which impacted Dominica in August 2007 (Smith et al. 2009b). Smith et al. (2009b) concluded that precipitation totals during Hurricane Dean were enhanced via the seeder–feeder effect, in which falling precipitation gathers additional cloud water from terrain-induced clouds over the high terrain, and increased the precipitation rate and rain accumulation on Dominica.

Regardless of whether forced mechanical lifting or the seeder–feeder effect is responsible, the climatological orographic enhancement of precipitation in trade wind flow and orographic enhancement of precipitation from Hurricane Dean’s rainbands both show a clear pattern of precipitation accumulation increasing with increasing elevation over Dominica’s mountains (Smith et al. 2009a,b, their Figs. 6 and 12, respectively).

No apparent trend of increasing rain amount or rain rate was found with increasing altitude in the case of TS Erika’s precipitation on Dominica. The far eastern and southern gauges closest to the coastline at lower elevations received the most precipitation from TS Erika (GF and GB in Fig. 2c). Other factors appear to have had a stronger influence on precipitation and will be discussed in the following section. While the expected pattern of orographic enhancement is not evident, Dominica’s mountains still played a role in modulating precipitation totals.

#### 4. Results

The time period of primary interest is the portion of TS Erika’s lifetime in closest proximity to Dominica, from 1200 UTC 26 August to 1200 UTC 28 August 2015. Observations of the environmental factors that affected the structure of TS Erika are described below.

##### a. Vertical wind shear

TS Erika was strongly affected by vertical wind shear during its lifetime. Strong vertical wind shear is hypothesized to be responsible for TS Erika’s decay (Pasch and Penny 2016). Vertical wind shear—commonly defined as the vector difference between 200 and 850 hPa—has been well studied in the prior literature and is one of the most important influential factors of tropical cyclone intensity (e.g., DeMaria and Kaplan 1999). This strong relationship is linked to the effects of vertical wind shear on tropical cyclone structure: shear tilts the vortex from its upright position (e.g., Jones 1995), organizes convection in the downshear half (in the direction of the shear vector; e.g.,

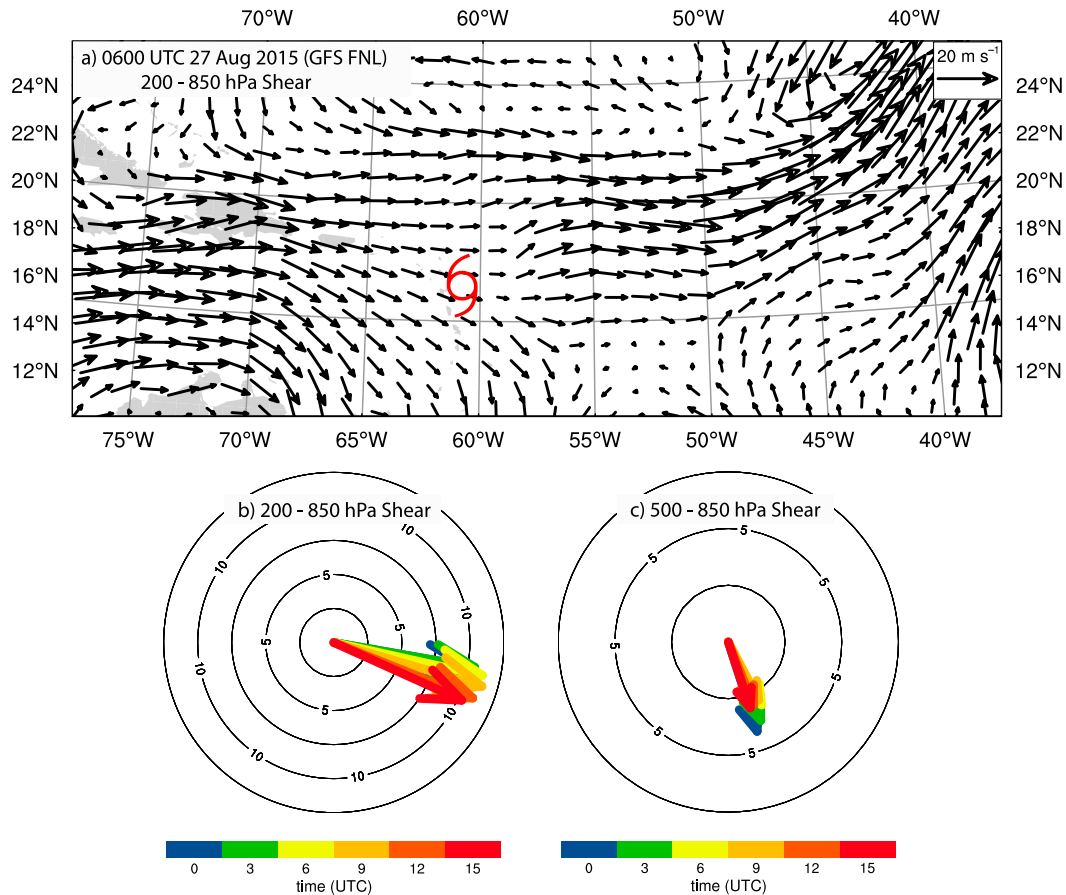


FIG. 4. (a) A map of the Caribbean basin (land areas are shaded) showing the environmental shear vectors (200–850 hPa) affecting TS Erika, with the storm motion removed at 0600 UTC 27 Aug 2015 from GFS FNL analyses. The location of TS Erika’s center is denoted by the hurricane symbol. Also included are 3-hourly snapshots of the (b) 200–850- and (c) 500–850-hPa environmental shear vector at 0000, 0300, 0600, 0900, 1200, and 1500 UTC on the same day, calculated as the average within 500 km of TS Erika’s center and color coded by the time. Rings represent shear magnitude in  $\text{m s}^{-1}$ ; note the change in scale between (b) and (c).

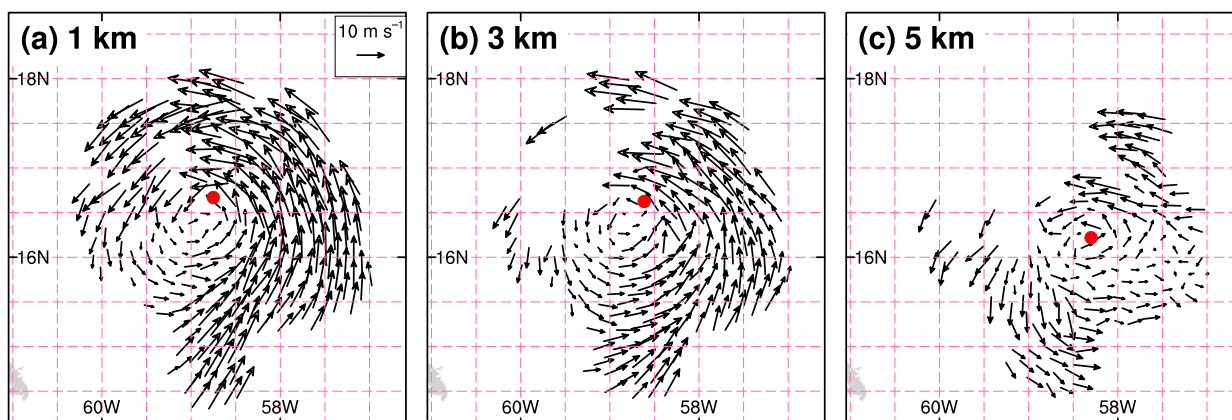
Corbosiero and Molinari 2002; Chen et al. 2006; Reasor et al. 2013), and provides pathways for dry air intrusions from the environment (e.g., Riemer and Montgomery 2011). A combination of vertical wind shear with other environmental factors (e.g., environmental humidity) can affect tropical cyclone structure and intensity changes (Rios-Berrios and Torn 2017). An assessment of the vertical wind shear affecting TS Erika is important in determining if shear played a role in organizing the heaviest precipitation south of the cyclone center.

Vertical wind shear was obtained from the Global Forecast System Final Analyses (GFS FNL; NOAA/NWS/NCEP/U.S. Department of Commerce 2015). To ensure that the shear vector represented the environment surrounding TS Erika, shear was calculated after removing the tropical cyclone vortex using the method of Galarneau and Davis (2013). To remove the vortex, the divergent and rotational wind components within a

prescribed radius (500 km, in this case) from the tropical cyclone center are subtracted from the total winds. Figure 4a shows the resulting 200–850-hPa environmental vertical wind shear affecting TS Erika as it approached Guadeloupe. Moderate-to-strong<sup>1</sup> west-northwesterly shear is evident just around and ahead of TS Erika. A closer look at the environmental shear was obtained by area-averaging the 200–850-hPa shear vector within a 500-km radius from the best track center of TS Erika (Fig. 4b), following the methods of statistical models for tropical cyclone intensity prediction (e.g., DeMaria and Kaplan 1999). Hourly depictions of the area-averaged shear vector from 0000 to 1500 UTC 27 August 2015 reveal that west-northwesterly shear

<sup>1</sup> See Rios-Berrios and Torn (2017) for definitions of moderate and strong shear based on statistical analyses.

2021 UTC 26 Aug 2015



0636 UTC 27 Aug 2015

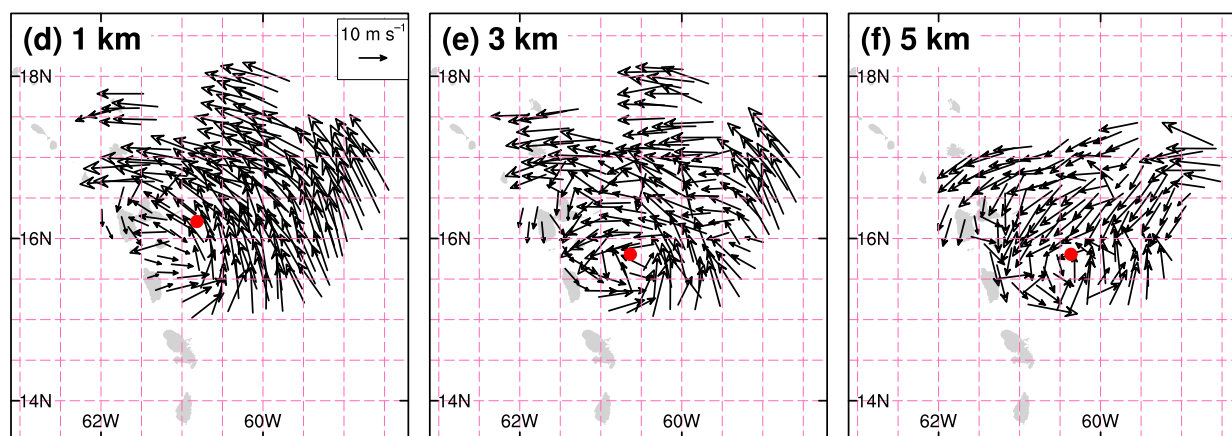


FIG. 5. Analysis of wind vectors from the TDR on board the P-3 aircraft. (a)–(c) Centered at 2021 UTC 26 Aug and (d)–(f) centered at 0636 UTC 27 Aug 2015. Three altitudes are shown: (left) 1, (middle) 3, and (right) 5 km, showing the shift in the rotation center with altitude. Gray shading denotes land area, red dots denote the circulation center at each level identified with a vorticity centroid approach, and a  $10 \text{ m s}^{-1}$  wind vector for reference is given in (a) and (d).

exceeded  $10 \text{ m s}^{-1}$  during the time of TS Erika's proximity to Dominica.

The deep-layer shear (200–850 hPa) is generally used to characterize wind shear around tropical cyclones. Figures 4a and 4b depict persistent west-northwesterly shear, which could cause the tropical cyclone vortex to become tilted toward the east-southeast. Vortex tilt was assessed through composite analysis of TDR winds at different vertical levels during the 26 August and 27 August missions (Fig. 5). A horizontal displacement of the vortex center with height is evident, as the 1-km center of circulation (Fig. 5a) was located toward the west-northwest with respect to the 3- and 5-km centers of circulation (Figs. 5b,c) on 26 August. The kinematic structure of TS Erika becomes largely asymmetric on 27 August, but the TDR analyses still suggest that the

1-km center of circulation is displaced from the 3- and 5-km centers of circulation.

To maintain thermal wind balance<sup>2</sup> in a tropical storm, the response of a tilted vortex consists of azimuthally asymmetric temperature and vertical motion anomalies (e.g., Raymond 1992; Jones 1995; DeMaria 1996). Cool anomalies appear in the downtilt region, whereas warm anomalies appear in the uptilt region. These thermal anomalies are established through adiabatic ascent and descent in the downtilt and uptilt regions, respectively

<sup>2</sup> Thermal wind balance is a dynamical balance resulting from hydrostatic and geostrophic balance, which relates horizontal temperature gradients to changes in horizontal wind with height (Holton 2004).



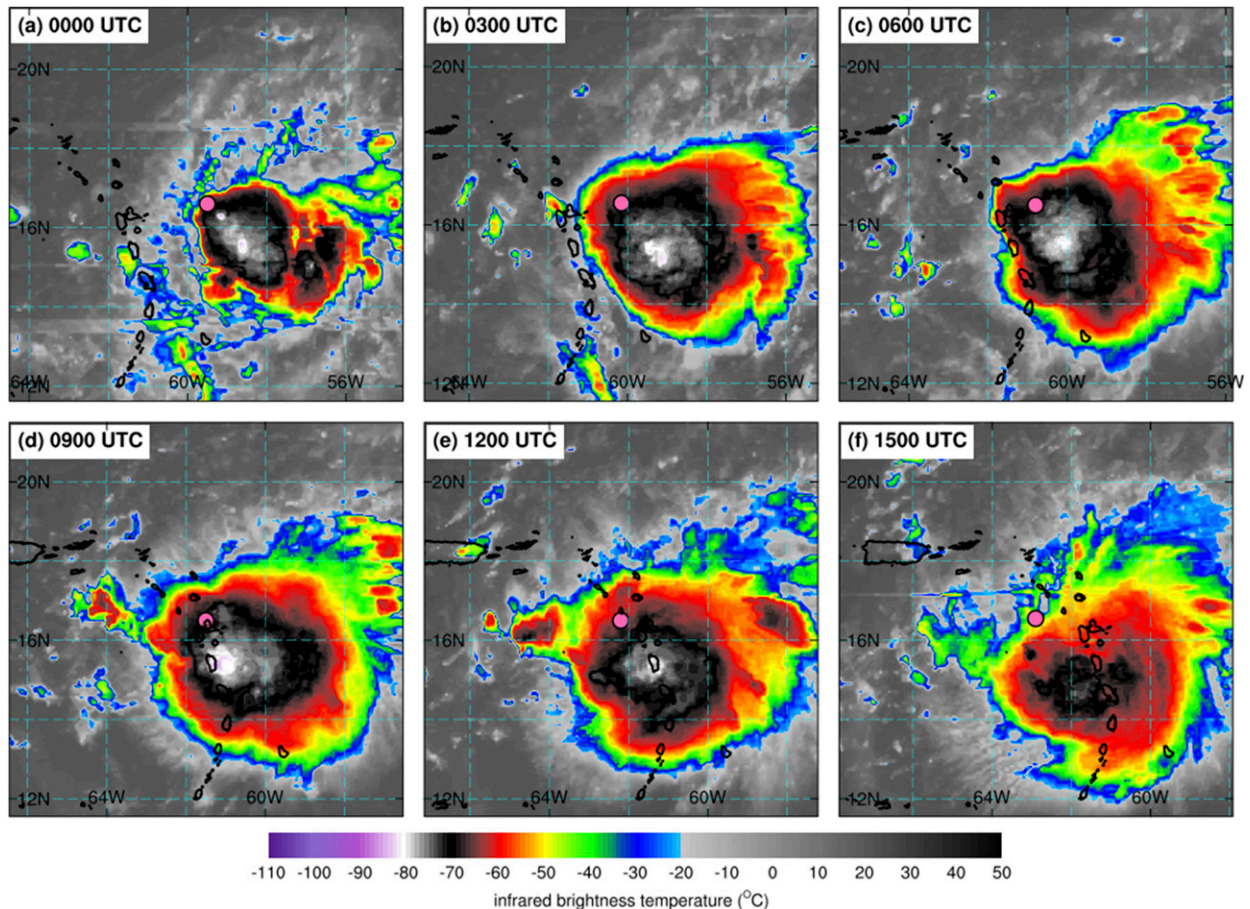


FIG. 6. (a)–(f) Storm-centered satellite images depicting infrared brightness temperature ( $^{\circ}\text{C}$ ) on 27 Aug 2015 from 0000 to 1500 UTC. Pink dots depict the interpolated 3-hourly best track position of TS Erika's center.

(Jones 1995). As a result of the anomalies, thermal instability is enhanced in the downtilt region and suppressed just above the surface center of circulation (DeMaria 1996). This is often referred to as “balanced lifting” or “mesoscale lifting” and can partially account for the enhanced convection in the downshear portion of TS Erika. Additionally, cooling aloft in the downshear region increases CAPE (Molinari et al. 2012), and lifting enables boundary layer air parcels to reach their level of free convection. Many studies found a similar pattern of enhanced convection in the downshear region of a tropical storm, with suppressed convection upshear (Corbosiero and Molinari 2002; Chen et al. 2006; Reasor et al. 2013; among others).

While there is some evidence for a tilted vortex in TS Erika based on the deep-layer shear, not all of the evidence is consistent with this picture. The convection from TS Erika was located to the south and east of the surface center of circulation, shown by the storm-centered GOES IR satellite images in Fig. 6. The pink dot represents the storm center, and brightness temperatures were brightest

(coldest) to the southeast of the dot. Convection toward the south and east of the center is also seen in Fig. 7a, where the hurricane symbol denotes the location of the low-pressure center, and the light shaded regions show the location of cloud cover. The colored portions of Fig. 7a show composite reflectivity from HAMSRS. Given the west-northwesterly deep-layer shear direction, the convective region should be located more toward the east than the south.

The tilted vortex structure with altitude looks somewhat different in the bottom row of Fig. 5 at the later time on 27 August 2015 than it does in the top row; the tilt appears to be meridionally oriented. The tilt direction, however, aligns well with the shallow shear from 500 to 850 hPa in Fig. 4c, showing a more north-northwesterly direction. The convective location toward the south and east of the surface center of circulation is consistent with the region of instability expected, based on a combination of the shallow and deep-layer shear patterns from Figs. 4b and 4c. This result suggests that the structure of TS Erika was more strongly influenced by the 500–850-hPa shear than the typically considered deep-layer shear. A

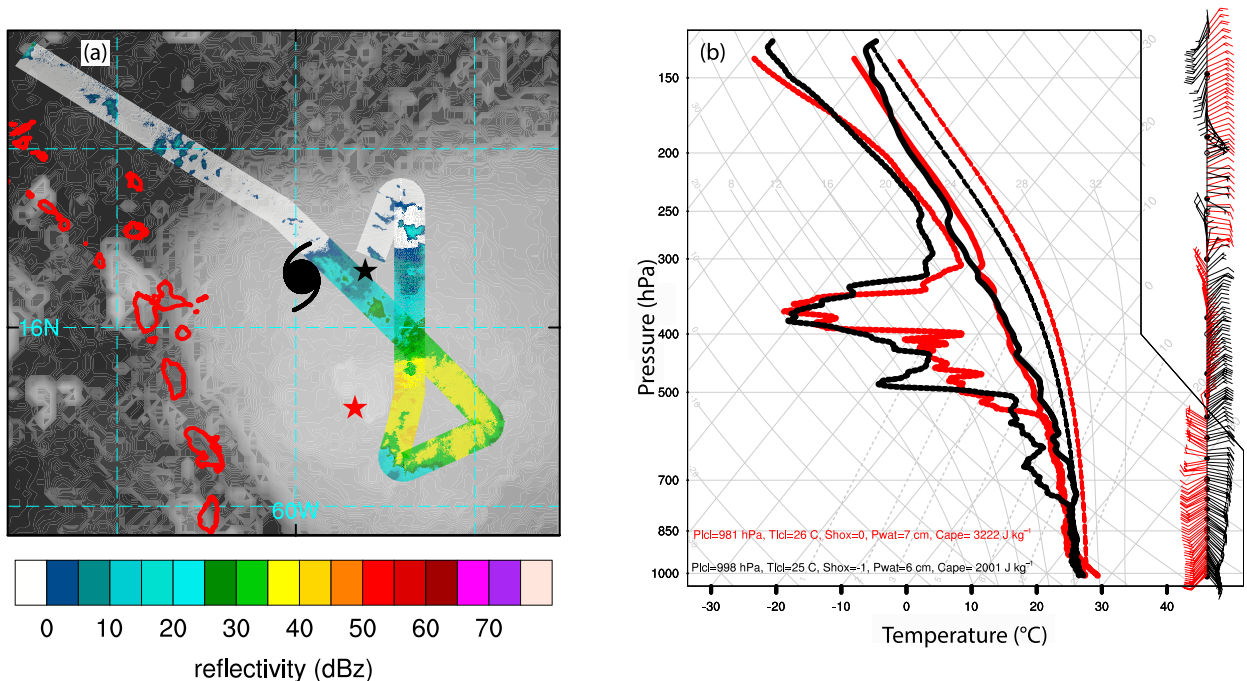


FIG. 7. (a) Storm-centered analysis of GOES infrared brightness temperature at 0300 UTC 27 Aug 2015 (gray shading) and HAMS composite reflectivity from 0100 to 0300 UTC 27 Aug 2015 (dBZ, color shading). The color-coded stars show the release locations of the dropwindsondes shown in (b), and the cyclone symbol shows the storm center interpolated from best track at 0300 UTC 27 Aug 2015. (b) Skew  $T$ -log $p$  diagrams from two dropwindsondes. The black (red) line shows the dropwindsonde dropped at 0443 UTC 27 Aug 2015 (0007 UTC 27 Aug 2015). Temperature (solid, center pair), dewpoint temperature (dotted, left pair), and the path of a surface-lifted parcel along a moist adiabat (dashed, right pair), are shown. Wind speed and direction are shown by wind vectors on the right, and common sounding indices ( $P_{LCL}$ ,  $T_{LCL}$ , Showalter index, precipitable water, and CAPE) are given along the bottom.

potential explanation for this result is that TS Erika was characterized by a shallow circulation extending only up to the midtroposphere. Evidence for this argument will be presented below and further discussed in section 5.

#### b. Dry northern sector

In addition to northwesterly shear, TS Erika evolved in an environment with relatively dry air to the north. The dry northern environment can be seen in atmospheric soundings from Global Hawk dropwindsondes. Figure 7b shows soundings from the two starred locations in Fig. 7a at 0443 UTC 27 August 2015 (black northern star) and 0007 UTC 27 August 2015 (red southern star). Both soundings in Fig. 7b have temperature profiles that follow along a moist adiabat much of the way through the troposphere. Both are saturated in the lower levels, up to  $\sim 750$  hPa, and have a relatively dry upper troposphere above  $\sim 550$  hPa. The vertical extent of the storm circulation appears to be limited to a rather shallow layer, as indicated by the aforementioned dry air above 550 hPa and the westerly winds south of TS Erika's center that appear only below 500 hPa. Note that more than two dropwindsondes were released from the

Global Hawk, but these two are representative of the northern and southern regions of the storm.

An important difference between soundings appears in the midlevels. The dropwindsonde that sampled the northern sector of the storm (black, Fig. 7b) captured a drier midtroposphere from 800 to 400 hPa, compared to the southern sector of the storm amid the convective region (red, Fig. 7b). The presence of dry air above 400 hPa in both soundings signals the presence of a dry air mass surrounding TS Erika. The soundings also portray differences in CAPE; the sounding in the northern sector measured less undiluted CAPE, or an atmosphere with more entrainment ( $2001 \text{ J kg}^{-1}$ ), than did the sounding in the southern sector ( $3222 \text{ J kg}^{-1}$ ). This is due, in part, to the higher boundary layer equivalent potential temperatures (as shown by the lifted parcel trace in the Fig. 7b soundings). Furthermore, the sounding in the northern sector shows subsidence, as temperature and dewpoint temperature inversions appear just above 800 hPa. Overall, these soundings indicate that the southern sector of TS Erika was more favorable for deep upward motions than was the northern sector.

While the northern dryness is apparent, the effects of the dryness on convective structure are less apparent.

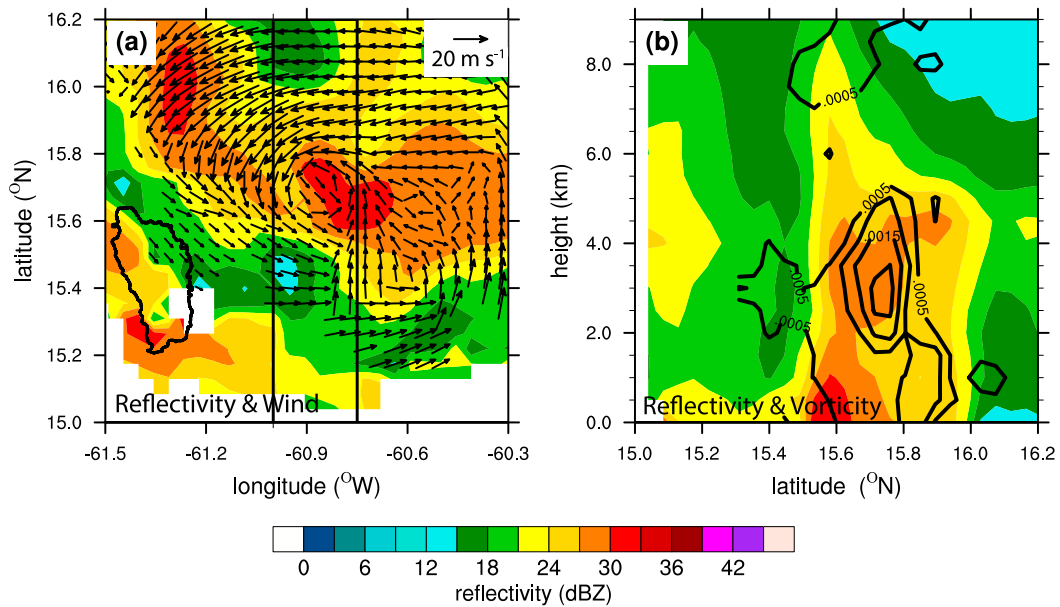


FIG. 8. (a) Wind speed and direction (vectors) and reflectivity (colors, dBZ) from the P-3 TDR showing a mesovortex south of the storm center and east of Dominica (outlined), centered at 0636 UTC 27 Aug 2015 at 3-km altitude. The highest reflectivities are associated with the center of low-level circulation. (b) A vertical cross section averaged between the two black lines in (a), showing vorticity with altitude (contours) and reflectivity (colors, dBZ).

Prior studies on moisture impacts on tropical cyclones have found that dry air can largely influence tropical cyclone intensification, depending on the vertical and horizontal distribution of the dry air (e.g., [Riemer et al. 2010](#); [Riemer and Montgomery 2011](#); [Tang and Emanuel 2012](#); [Ge et al. 2013](#); [Wu et al. 2015](#); [Rios-Berrios and Torn 2017](#)). Sheared tropical cyclones, in particular, are less likely to intensify when dry air is present in the mid-troposphere and in the upshear half ([Rios-Berrios and Torn 2017](#)). In the case of TS Erika, dry air was present to the north and west, or upshear per the 200–850-hPa shear vector, of the surface center of TS Erika. TS Erika was originally forecast to intensify, but this dry region could have prevented intensification. On the other hand, the combination of upshear dryness and shear-induced asymmetric vertical motions could have prevented convective development to the north and enhanced convective development to the south by delaying the onset of convection. The actual effect on TS Erika remains uncertain from limited observations, but a potential enhancement effect of the dryness will be further discussed in [section 5](#).

### c. Mesovortex

The final unique aspect of TS Erika that merits a thorough description and discussion is the presence of a circulation center exclusive from the main vortex that can be seen in multiple radar observations. This feature is referred to as a mesovortex due to its mesoscale size

(on the order of 100 km) and its cyclonic rotating motion. Approximately 100 km south of the storm center, the mesovortex is first apparent in observations at 0636 UTC 27 August 2015 in the TDR velocities from the NOAA P-3 aircraft in [Fig. 8a](#). The circulation feature is coincident with high radar reflectivities just to the east-northeast of Dominica. Wind speeds in the mesovortex are around 10–15 m s<sup>-1</sup>, rotating counterclockwise.

The vertical structure of the mesovortex is shown in [Fig. 8b](#), with a cross section averaged between the two black lines in [Fig. 8a](#). The mesovortex appears to be focused above the surface, as indicated by the largest vorticity values, which are found around 3-km altitude. Positive vorticity values extend from the surface through 5 km, showing the robustness and developed nature of the mesovortex. Moreover, the mesovortex appears linked to a convective cell, as indicated by reflectivity values exceeding 20 dBZ in the vicinity of large and positive relative vorticity. The downshear half of sheared TCs is typically characterized by large CAPE, helicity, and vortex stretching ([Molinari and Vollaro 2010](#); [Nguyen 2015](#)), which supports the formation of mesoscale vortices within that region ([Molinari et al. 2006](#); [Nguyen 2015](#)). Based on this evidence, it is possible that the mesovortex shown in [Fig. 8](#) formed within the shear-organized convection.

About 2 h later, as the mesovortex approaches Dominica, a circulation center can be observed by the S-band Météo-France radar on Guadeloupe. The

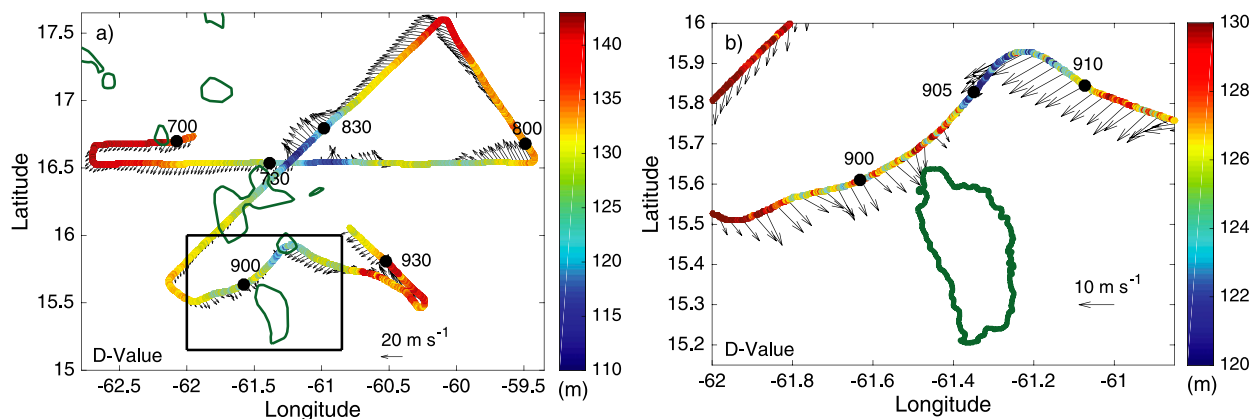


FIG. 9.  $D$ -value (m, color), flight-level wind ( $\text{m s}^{-1}$ , vectors), and a few times (UTC) are shown from the NOAA P-3 on 27 Aug 2015 from about 3-km altitude. (a) A larger portion of the flight where TS Erika's storm center can be distinguished from the mesovortex center and (b) zoomed in on just Dominica and the mesovortex. Note the change in vector scale and  $D$ -value color scale from (a) to (b).

Météo-France Guadeloupe radar is not dual Doppler, but radar-tracked features from the method described in section 2b show cyclonic motion that persists near Dominica for over 5 h (Fig. 3), from 0830 to 1400 UTC 27 August 2015. In addition to the cyclonic motion in Fig. 3, also included are the 1-hourly precipitation totals, which show that the cyclonic feature was accompanied by heavy precipitation for the duration of its existence. The circulation features seen in Figs. 3 and 8 are not associated with the main circulation of TS Erika, which is clearly north of this feature by about 100 km. Evidence for this is provided by the flight-level winds in Fig. 9a and the  $D$ -value discussed in the following paragraph.

The cyclonic feature is found to be coincident with low  $D$ -values (Fig. 9);  $D$ -values were obtained from flight-level data during the 27 August NOAA P-3 mission. A  $D$ -value denotes the difference between the actual height and the standard atmospheric height of a constant-pressure surface. Thus, a small  $D$ -value relative to the nearby surroundings can be representative of a low-pressure center (Parish et al. 2016). The P-3 aircraft flew through the mesovortex a little after 0900 UTC at 3-km altitude, just before the mesovortex reached Dominica. In Fig. 9a, the lower  $D$ -values from TS Erika's center are seen as a separate entity, well north of the low  $D$ -values associated with the mesovortex near Dominica. A zoomed-in view near Dominica is shown in Fig. 9b. The  $D$ -value evidence tells us that not only does the mesovortex have cyclonic rotation and vorticity, but it is also a low-pressure feature. In addition to low  $D$ -values and low pressure, the same P-3 dataset shows that the mesovortex also has a relatively warm and moist center, with some sporadic vertical velocities (not shown).

With the combination of Figs. 8a and 3a–c, the mesovortex can be observed moving westward from 0636 UTC, when the mesovortex is seen east of Dominica by

the TDR, and from 0830 to 0930 UTC, where it is seen east of Dominica but closer to the island. From 1000 to 1230 UTC (Figs. 3d–i), the mesovortex stays fixed over Dominica, and the high precipitation totals coincide with this time period (Fig. 2a). After 1300 UTC, the mesovortex can again be seen moving westward, this time away from Dominica (Figs. 3j–l).

Using best track coordinates for the surface low-pressure center of TS Erika, the translation speed of the storm can be estimated and compared against the translation speed of the mesovortex. The average translation speed of TS Erika on 27 August 2015 was  $23.6 \text{ km h}^{-1}$ , computed from best track data. Using the approximate location of the mesovortex in Fig. 8 (15.7°N, 60.8°W) at 0636 UTC and the approximate location of the mesovortex in Fig. 3a (15.7°N, 61.2°W) at 0830 UTC, the translation speed before it reached Dominica was  $23.4 \text{ km h}^{-1}$ , which matches well with the storm translation speed. If the mesovortex had maintained this speed, it would have passed Dominica in less than 1 h. Instead, it spent over 3 h centered on Dominica (Figs. 3d–i) as a quasi-stationary feature. In addition, assuming a straight path between the two locations above, the mesovortex would have passed to the north of Dominica.

## 5. Discussion and conclusions

The center of TS Erika passed over the northern coast of Guadeloupe on 27 August 2015 (Fig. 1). Dominica, to the south, received over 500 mm of precipitation in about 5 h (Fig. 2), while precipitation on Guadeloupe was unexceptional. As TS Erika was developing, it entered into a region with strong west-northwesterly deep-layer shear (Fig. 4) that affected the storm's

development and structure. The sheared environment caused vortex tilt (Fig. 5) and the associated downshear convection and precipitation typical of sheared tropical cyclones (Figs. 6, 7a). Dropwindsonde observations show a region with drier air and some subsidence in the northern portion of TS Erika (Fig. 7b). Unfortunately, it was the downshear region with enhanced convection that passed directly over Dominica. Furthermore, a cyclonic circulation (on the scale of  $\sim 100$ -km diameter,  $10\text{--}15\text{ m s}^{-1}$ ) was embedded within the TS (Figs. 3, 8, 9). This mesovortex was observed just to the east of Dominica by the TDR. It migrated westward and was later observed over Dominica by the Guadeloupe Météo-France radar in tracked features. There, it persisted for 3 h, directly over Dominica, causing continuous and heavy rain over the island and contributing to the heavy rain totals.

A number of factors were influential in the heavy precipitation Dominica received from TS Erika. The role of the storm environment and the mesovortex will be further discussed below. The reason TS Erika impacted Dominica so strongly and the atypical nature of the event will also be discussed.

#### *a. Factors contributing to heavy precipitation*

##### 1) STORM ENVIRONMENT

The primary factor responsible for the heavy precipitation on Dominica was the tropical storm environment. The mechanism for wind shear enhancement of downshear convection was discussed in section 4a. But the importance of the circulation depth and combined importance of the wind shear and dry northern sector of the storm deserve further elaboration.

With regard to the circulation depth, the evidence presented in this study suggests the following:

- The enhanced convective region to the south of TS Erika was more consistent with the north-northwesterly shallow-layer shear (500–850 hPa) than the west-northwesterly deep-layer shear (200–850 hPa) discussed in section 4a.
- While the deep-layer shear is traditionally used with respect to tropical cyclones, in the case of TS Erika, this was misleading because the shallow shear was more relevant.
- TS Erika's circulation was relatively shallow and weak, demonstrating that a shallow-layer shear is more applicable to a weak tropical cyclone like TS Erika than to strong tropical cyclones.
- Because of the shallow and weak nature of TS Erika and the shallow north-northwesterly shear, Dominica to the south received the core of precipitation from the storm.

These results reveal that the location of the heaviest rainfall could have been better predicted with a combined assessment of vertical wind shear between deep and shallow layers and the vertical structure of TS Erika.

In addition to the circulation depth, a convective strengthening mechanism, based on a combination of the patterns of environmental shear and moisture, also played a role. The dry upshear environment to the north of TS Erika prevented convection by diluting updrafts both through entrainment (due to the dryness) and through subsidence (due to the shear), which increased static stability (e.g., James and Markowski 2010; Kilroy and Smith 2013; Molinari et al. 2012). Imagine a surface air parcel moving counterclockwise around a tropical cyclone, beginning on the upshear side. As it advects around the surface center, the parcel gains heat and moisture and is continuously ripening for convection. But, given the increased stability, convection does not yet occur. As this parcel continues to advect cyclonically around the storm center, it soon enters the downshear region. Already more than ready to convect with ample heat and moisture, it is finally able to lift along the lifted potential temperature surfaces and release its energy into the convective region downshear. This mechanism was documented with air parcel trajectories for a sheared tropical cyclone (Nguyen 2015), and intense downshear convective bursts have been discussed in the literature associated with weak, sheared tropical cyclones (e.g., DeMaria et al. 2012; Fierro and Mansell 2017). Despite the compelling observational evidence, further investigation is needed to confirm the role of this convective enhancement mechanism within TS Erika.

##### 2) MESOVORTEX

Another additive element to TS Erika's heavy precipitation on Dominica was the mesovortex that formed and moved over the high terrain of the island. The heaviest rain rates and highest rainfall accumulations occurred during this time period. The mesovortex was observed in multiple ways and from a number of platforms and instruments. The effort here is to consolidate all of the lines of evidence for the existence of the mesovortex into one diagram (Fig. 10).

The mesovortex was first observed at 0636 UTC 27 August 2015 by the TDR aboard the P-3 (Fig. 8). This is the first and the best look because the TDR directly measures reflectivity, as well as Doppler velocity, from which vorticity can be computed. From Fig. 8, the mesovortex is estimated to be  $\sim 1^\circ$  in diameter ( $\sim 110$  km) and extends from the surface up to 5-km altitude, with associated reflectivity as high as 9 km. The approximate location, based on Fig. 8, is shown in Fig. 10 and labeled with the time observed.

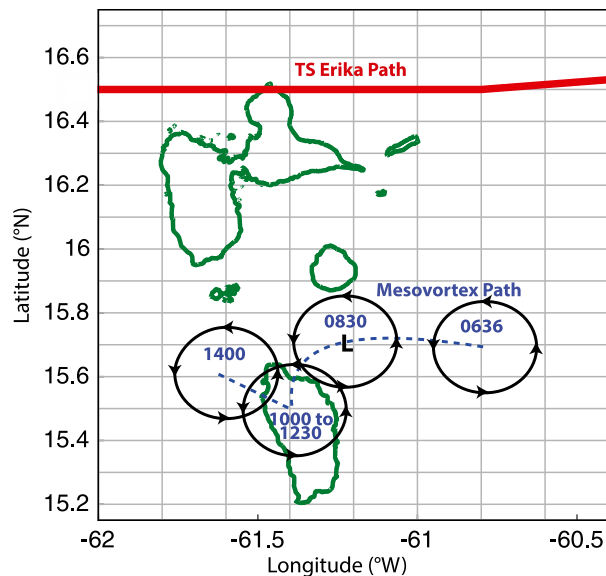


FIG. 10. A diagram showing the observed path of the mesovortex, citing the approximate location and time (UTC) it was observed by various observational platforms with a map of the nearby islands (green lines) in the background for reference, along with the best track path of TS Erika (red line).

The next time the mesovortex was well observed was from 0830 to 0930 UTC by the radar-tracked reflectivity features from the operational Météo-France Guadeloupe radar (Fig. 3, top row). The L in Fig. 10 denotes that just after 0900 UTC, a small *D*-value, indicating a low-pressure center, was observed in situ by the NOAA P-3 aircraft (Fig. 9), coincident in time and space with the observations from the radar-tracked features. The mesovortex then persisted over the terrain of Dominica for over 2 h before heading toward the northwest, where it was last seen by the radar at 1400 UTC (Fig. 10).

Observational evidence points to two unique aspects of the mesovortex: its movement toward and its persistence over Dominica. Assuming it was traveling in a straight line from when it was observed at 0636 to 0830 UTC, it is surprising that it moved southward to where it centered over the northern portion of Dominica. Tropical cyclone track changes associated with orography have been extensively studied in Taiwan (e.g., Wu and Kuo 1999; Lin et al. 2005), and one study shows that Taiwan's topography sometimes attracts vortices when they pass to the north (Huang et al. 2011). The mechanism for track modification near mountains is due to mesoscale channeling wind effects and is sensitive to the exact topography, storm approach direction, wind speed, and storm translation speed (Huang et al. 2011). The mesovortex in this case is much smaller, with shallower circulation than most typhoons near Taiwan; Dominica also has a much smaller land area and shorter terrain heights than Taiwan. Still,

based on the general dynamics of mesovortex interactions with terrain, the hypothesis is as follows: when the cyclonically rotating mesovortex approached the northern part of Dominica, westerly winds from the mesovortex reached the terrain and caused air to accumulate on the northwest side, causing local positive pressure. On the opposite northeast side of Dominica, air evacuated at low levels with little replacement because of terrain blockage, causing a local pressure minimum. This effect could cause the low pressure of the mesovortex to shift toward the induced low pressure on Dominica instead of passing to the north. A similar mechanism is associated at synoptic scales with lee cyclogenesis over the Rockies, termed an “amoebalike” movement (Bannon 1992).

The second unique aspect of the mesovortex is its persistence and quasi stationarity over Dominica. In section 4c, the translation speed of the mesovortex and TS Erika's center were found to be nearly the same until the mesovortex encountered Dominica, at which point it drastically slowed. The stationarity of the mesovortex over Dominica was driven by a classic positive feedback: a low pressure disturbance draws air toward its center, where the air converges and lifts, and water vapor condenses, releasing latent heat and enhancing vertical lifting, which reinforces the initial surface low. In this case, the mesovortex is the initial low-pressure disturbance, and orographic lifting adds to the vertical motion. The main difference is the stationarity of the orography influencing the location of the updrafts and keeping the mesovortex centered over the island.

Observational evidence is limited for both the mesovortex movement toward Dominica and its persistence over Dominica. Open questions remain, but future numerical modeling tests can help confirm the mesovortex hypotheses. Despite remaining unknowns, the strong focus on the mesovortex in this manuscript is due to its relationship with precipitation on Dominica. Much of the precipitation on Dominica fell during the time of the mesovortex, and its extensive temporal duration over the island was a strong factor in enhancing the quantity of precipitation from TS Erika.

### 3) OROGRAPHY

It is clear that Dominica's terrain played a role in the precipitation on Dominica (see Figs. 2a, 3), but it was not a typical orographic effect (see Houze 2012). The mesovortex would have advected with the mean flow of TS Erika had Dominica not been present. Therefore, while Dominica's terrain was not responsible for the formation of the mesovortex, its primary role was in attracting and maintaining the mesovortex over the island. The mesovortex, and the unusual situation it brought to Dominica, was responsible for the lack of a

TABLE 1. Top 10 rain events on Dominica from the TMPA climatology, ranked by amount in the years 1998–2015. The rank, 24-h precipitation accumulation (mm), event date, and name are given.

Rank	24-h precipitation (mm)	Date	Event (if named)
1	197.4	27 Aug 2015	TS Erika (2015)
2	158.7	29 Jul 2001	
3	150.9	10 Sep 2007	
4	150.7	3 Sep 2009	TS Erika (2009)
5	147.7	28 Nov 2011	
6	145.1	17 Aug 2007	Hurricane Dean (2007)
7	142.6	18 Jun 2003	
8	139.0	8 Nov 2014	
9	135.4	21 Nov 2004	
10	135.1	19 Nov 1999	TS Lenny (1999)

typical orographic precipitation enhancement signature from TS Erika. While observations alone cannot confirm the above statements, future modeling efforts can isolate the role of terrain on precipitation from this event.

*b. Impacts on Dominica*

Dominica had experienced heavy rainfall events in the past, but TS Erika was the highest 24-h precipitation accumulation event in the time period covering 1998–2015. Table 1 shows the top 10 rain events from TRMM’s Multiplatform Precipitation Analysis (TMPA) climatology, a blend between low-orbit microwave satellites and geostationary IR satellites (Huffman et al. 2007). The analysis was computed as an average over the two 0.25° × 0.25° grid points centered on Dominica. Rainfall for TS Erika (2015, not to be confused with 2009) on Dominica is underestimated due to satellite estimation and grid box averaging. However, TS Erika was still record breaking (Table 1).

Four of the top 10 rainfall events on Dominica were associated with tropical cyclones (three tropical storms and one hurricane; Table 1). A similar analysis of rainfall from TMPA, associated with only tropical cyclones,

was also done for cyclones that passed within 500 km of Dominica (Table 2). In that analysis, eight of the 10 top rainfall events were from tropical storms or depressions (D), while only two were hurricanes. This analysis clearly shows that while TS Erika was a significant and record-breaking rain event for Dominica, extreme rainfall from a tropical storm (as opposed to a hurricane) is not surprising in that region.

Hurricane Dean (2007) makes both top 10 lists. Four of the same rain gauges recorded precipitation totals from 155 to 517 mm from Hurricane Dean, highly dependent on the altitude and east–west placement of the rain gauge (Smith et al. 2009b). This type of clear orographic precipitation pattern was initially expected from TS Erika and is one of the reasons precipitation on Dominica from TS Erika was unusual.

Precipitation accumulations from TS Erika on Dominica do not appear to be orographically controlled in the traditional sense. Low-elevation gauges near the east and southern coast received just as much rain as did high-elevation, mountaintop gauges, and it did not seem to matter where the gauge was located. The spatial coverage of precipitation from TS Erika was remarkable. It moved large boulders, diverted rivers, and caused landslides (Ogden 2016). The torrential rain also displaced entire towns; the southern rain gauge site at Grand Bay, with the second most cumulative precipitation from TS Erika, was located near two of the permanently displaced towns (Petite Savanne and Dubique).

Tropical storm watches and warnings are based exclusively on wind speed probabilities, not precipitation probabilities. TS Erika was not a strong storm from a wind perspective. Tropical storm warnings were issued by the National Hurricane Center for many islands north of Dominica along TS Erika’s forecasted projected path. These included Guadeloupe (watch only), Anguilla, Saba, St. Eustatius, St. Maarten, Antigua, Barbuda, Montserrat,

TABLE 2. Top 10 rain events on Dominica from cyclones passing within 500 km. Data are from the TMPA climatology, ranked by amount in the years 1998–2015. The rank, 24-h precipitation accumulation (mm), event date, tropical cyclone name, intensity (kt and category), and closest approach to Dominica (km) are given. H1, hurricane category 1; H4, hurricane category 4; D, tropical depression.

Rank	24-h precipitation (mm)	Date	Tropical cyclone	Intensity (kt and category)	Closest approach (km)
1	197.4	27 Aug 2015	Erika (2015)	45 (TS)	140
2	150.7	3 Sep 2009	Erika (2009)	40 (TS)	182
3	145.1	17 Aug 2007	Dean (2007)	90 (H1)	114
4	135.1	19 Nov 1999	Lenny (1999)	60 (TS)	275
5	113.5	22 Aug 2012	Isaac (2012)	45 (TS)	132
6	107.4	14 Sep 2004	Jeanne (2004)	25 (D)	100
7	94.2	13 Oct 2012	Rafael (2012)	35 (TS)	200
8	93.9	16 Oct 2008	Omar (2008)	115 (H4)	414
9	91.6	15 Aug 2004	Earl (2004)	35 (TS)	396
10	75.0	1 Aug 2014	Bertha (2014)	45 (TS)	151

St. Kitts, Nevis, Puerto Rico, U.S. and British Virgin Islands, St. Barthélemy, Dominican Republic, Haiti, Turks and Caicos, and the Bahamas (all had watches upgraded to warnings) (Pasch and Penny 2016). In terms of wind forecasting, this was appropriate. The strongest winds recorded on Dominica were only 34 kt (Pasch and Penny 2016). Even Guadeloupe, which bore a direct hit from the surface low-pressure center of TS Erika, only saw wind gusts as high as 52 kt (Pasch and Penny 2016).

Forecast precipitation amounts for Dominica, as well as all global model ensemble forecasts, were well below the actual precipitation accumulations received. While it is not surprising that coarse-resolution global models underpredict precipitation on small islands, the stark contrast between predicted and actual rainfall amounts shows how little warning came before the event to the people on Dominica. The early-morning timing and unexpected nature of the event meant that little preparation or precaution was taken. Furthermore, poor precipitation forecasts lend further evidence to the idea that the mesovortex interaction with orography, something certainly unresolved by models, played a significant role.

TS Erika is a good reminder that just because an area is not under a tropical storm watch or warning, it does not mean the threat of a natural hazard is negligible. Flooding and landslides resulted from the heavy precipitation discussed in section 3, but the heavy precipitation was partially caused by the mesovortex discussed in section 4c. A transient, mesoscale feature like the mesovortex is extremely difficult to model and even more difficult to predict or forecast, especially in a region with complex terrain. Hopefully, this case study can bring a greater focus to the dangers of heavy precipitation from all types of tropical storms and serve as a learning experience to help mitigate the loss of lives and property and prepare for extreme rainfall events in the future.

*Acknowledgments.* The authors thank Marshall Alexander first and foremost for maintaining the rain gauge transect on Dominica and regularly collecting the data, even in difficult conditions. The authors also thank Prof. Fred Ogden for the radar data processing and analysis, Dr. Michael Dixon for the radar-tracked winds, Prof. Ryan Torn for support of all types, and Dr. Leon Nguyen for brainstorming and idea development. Aircraft data from the NOAA missions were obtained from the NOAA HRD website ([www.aoml.noaa.gov/hrd](http://www.aoml.noaa.gov/hrd)). Prof. Alison D. Nugent was partially supported by NSF AGS Grant PRF 1431053, and Dr. Rosimar Rios-Berrios was supported by NOAA Grant NA14OAR4830172 and the NCAR Advanced Study Program Graduate Student Visitor program. NCAR is funded by the National Science Foundation and managed by the University Corporation for Atmospheric Research.

## REFERENCES

- Bannon, P., 1992: A model of Rocky Mountain lee cyclogenesis. *J. Atmos. Sci.*, **49**, 1510–1522, [https://doi.org/10.1175/1520-0469\(1992\)049<1510:AMORML>2.0.CO;2](https://doi.org/10.1175/1520-0469(1992)049<1510:AMORML>2.0.CO;2).
- Brown, S. T., B. Lambriksen, R. F. Denning, T. Gaier, P. Kangaslahti, B. H. Lim, J. M. Tanabe, and A. B. Tanner, 2011: The High-Altitude MMIC Sounding Radiometer for the Global Hawk unmanned aerial vehicle: Instrument description and performance. *IEEE Trans. Geosci. Remote Sens.*, **49**, 3291–3301, <https://doi.org/10.1109/TGRS.2011.2125973>.
- Chen, S. S., J. A. Knaff, and F. D. Marks Jr, 2006: Effects of vertical wind shear and storm motion on tropical cyclone rainfall asymmetries deduced from TRMM. *Mon. Wea. Rev.*, **134**, 3190–3208, <https://doi.org/10.1175/MWR3245.1>.
- Corbosiero, K., and J. Molinari, 2002: The effects of vertical wind shear on the distribution of convection in tropical cyclones. *Mon. Wea. Rev.*, **130**, 2110–2123, [https://doi.org/10.1175/1520-0493\(2002\)130<2110:TEOVWS>2.0.CO;2](https://doi.org/10.1175/1520-0493(2002)130<2110:TEOVWS>2.0.CO;2).
- DeMaria, M., 1996: The effect of vertical shear on tropical cyclone intensity change. *J. Atmos. Sci.*, **53**, 2076–2088, [https://doi.org/10.1175/1520-0469\(1996\)053<2076:TEOVSO>2.0.CO;2](https://doi.org/10.1175/1520-0469(1996)053<2076:TEOVSO>2.0.CO;2).
- , and J. Kaplan, 1999: An updated Statistical Hurricane Intensity Prediction Scheme (SHIPS) for the Atlantic and Eastern North Pacific basins. *Wea. Forecasting*, **14**, 326–337, [https://doi.org/10.1175/1520-0434\(1999\)014<0326:AUSHIP>2.0.CO;2](https://doi.org/10.1175/1520-0434(1999)014<0326:AUSHIP>2.0.CO;2).
- , R. T. DeMaria, J. A. Knaff, and D. Molenaar, 2012: Tropical cyclone lightning and rapid intensity change. *Mon. Wea. Rev.*, **140**, 1828–1842, <https://doi.org/10.1175/MWR-D-11-00236.1>.
- Dixon, M., and G. Wiener, 1993: TITAN: Thunderstorm Identification, Tracking, Analysis, and Nowcasting—A radar-based methodology. *J. Atmos. Oceanic Technol.*, **10**, 785–797, [https://doi.org/10.1175/1520-0426\(1993\)010<0785:TTITAA>2.0.CO;2](https://doi.org/10.1175/1520-0426(1993)010<0785:TTITAA>2.0.CO;2).
- Dolling, K. P., and G. M. Barnes, 2012: The creation of a high equivalent potential temperature reservoir in Tropical Storm Humberto (2001) and its possible role in storm deepening. *Mon. Wea. Rev.*, **140**, 492–505, <https://doi.org/10.1175/MWR-D-11-00068.1>.
- Fierro, A. O., and E. R. Mansell, 2017: Electrification and lightning in idealized simulations of a hurricane-like vortex subject to wind shear and sea surface temperature cooling. *J. Atmos. Sci.*, **74**, 2023–2041, <https://doi.org/10.1175/JAS-D-16-0270.1>.
- Galarneau, T. J., and C. A. Davis, 2013: Diagnosing forecast errors in tropical cyclone motion. *Mon. Wea. Rev.*, **141**, 405–430, <https://doi.org/10.1175/MWR-D-12-00071.1>.
- Ge, X., T. Li, and M. Peng, 2013: Effects of vertical shears and midlevel dry air on tropical cyclone developments. *J. Atmos. Sci.*, **70**, 3859–3875, <https://doi.org/10.1175/JAS-D-13-066.1>.
- Hock, T. F., and J. L. Franklin, 1999: The NCAR GPS dropwindsonde. *Bull. Amer. Meteor. Soc.*, **80**, 407–420, [https://doi.org/10.1175/1520-0477\(1999\)080<0407:TNGD>2.0.CO;2](https://doi.org/10.1175/1520-0477(1999)080<0407:TNGD>2.0.CO;2).
- Holton, J. R., 2004: *An Introduction to Dynamic Meteorology*. 4th ed. International Geophysics Series, Vol. 88, Elsevier Academic Press, 535 pp.
- Houze, R. A., 2012: Orographic effects on precipitating clouds. *Rev. Geophys.*, **50**, RG1001, <https://doi.org/10.1029/2011RG000365>.
- Huang, Y.-H., C.-C. Wu, and Y. Wang, 2011: The influence of island topography on typhoon track deflection. *Mon. Wea. Rev.*, **139**, 1708–1727, <https://doi.org/10.1175/2011MWR3560.1>.
- Huffman, G. J., and Coauthors, 2007: The TRMM Multisatellite Precipitation Analysis (TMPA): Quasi-global, multiyear,



- combined-sensor precipitation estimates at fine scales. *J. Hydrometeorol.*, **8**, 38–55, <https://doi.org/10.1175/JHM560.1>.
- James, R. P., and P. M. Markowski, 2010: A numerical investigation of the effects of dry air aloft on deep convection. *Mon. Wea. Rev.*, **138**, 140–161, <https://doi.org/10.1175/2009MWR3018.1>.
- Jones, S. C., 1995: The evolution of vortices in vertical shear. I: Initially barotropic vortices. *Quart. J. Roy. Meteor. Soc.*, **121**, 821–851, <https://doi.org/10.1002/qj.49712152406>.
- Jorgensen, D. P., P. H. Hildebrand, and C. L. Frush, 1983: Feasibility test of an airborne pulse-Doppler meteorological radar. *J. Climate Appl. Meteorol.*, **22**, 744–757, [https://doi.org/10.1175/1520-0450\(1983\)022<0744:FTOAAAP>2.0.CO;2](https://doi.org/10.1175/1520-0450(1983)022<0744:FTOAAAP>2.0.CO;2).
- Kilroy, G., and R. K. Smith, 2013: A numerical study of rotating convection during tropical cyclogenesis. *Quart. J. Roy. Meteor. Soc.*, **139**, 1255–1269, <https://doi.org/10.1002/qj.2022>.
- Lin, Y.-L., S.-Y. Chen, C. M. Hill, and C.-Y. Huang, 2005: Control parameters for the influence of a mesoscale mountain range on cyclone track continuity and deflection. *J. Atmos. Sci.*, **62**, 1849–1866, <https://doi.org/10.1175/JAS3439.1>.
- Lonfat, M., F. D. Marks Jr., and S. S. Chen, 2004: Precipitation distribution in tropical cyclones using the Tropical Rainfall Measuring Mission (TRMM) microwave imager: A global perspective. *Mon. Wea. Rev.*, **132**, 1645–1660, [https://doi.org/10.1175/1520-0493\(2004\)132<1645:PDITCU>2.0.CO;2](https://doi.org/10.1175/1520-0493(2004)132<1645:PDITCU>2.0.CO;2).
- Lorsolo, S., J. Zhang, F. Marks, and J. Gamache, 2010: Estimation and mapping of hurricane turbulent energy using airborne Doppler measurements. *Mon. Wea. Rev.*, **138**, 3656–3670, <https://doi.org/10.1175/2010MWR3183.1>.
- Minder, J. R., R. B. Smith, and A. D. Nugent, 2013: The dynamics of ascent-forced orographic convection in the tropics: Results from Dominica. *J. Atmos. Sci.*, **70**, 4067–4088, <https://doi.org/10.1175/JAS-D-13-016.1>.
- Molinari, J., and D. Vollaro, 2010: Distribution of helicity, CAPE, and shear in tropical cyclones. *J. Atmos. Sci.*, **67**, 274–284, <https://doi.org/10.1175/2009JAS3090.1>.
- , P. Dodge, D. Vollaro, K. L. Corbosiero, and F. Marks, 2006: Mesoscale aspects of the downshear reformation of a tropical cyclone. *J. Atmos. Sci.*, **63**, 341–354, <https://doi.org/10.1175/JAS3591.1>.
- , D. M. Romps, D. Vollaro, and L. Nguyen, 2012: CAPE in tropical cyclones. *J. Atmos. Sci.*, **69**, 2452–2463, <https://doi.org/10.1175/JAS-D-11-0254.1>.
- NOAA/NWS/NCEP/U.S. Department of Commerce, 2015: NCEP GDAS/FNL 0.25 degree global tropospheric analyses and forecast grids. Research Data Archive at the National Center for Atmospheric Research, Computational and Information Systems Laboratory, accessed 1 June 2016, <https://rda.ucar.edu/datasets/ds083.3/>.
- Nguyen, L. T., 2015: The intensification of sheared tropical cyclones. Ph.D. thesis, State University of New York at Albany, 175 pp.
- Nugent, A. D., R. B. Smith, and J. R. Minder, 2014: Wind speed control of tropical orographic convection. *J. Atmos. Sci.*, **71**, 2695–2712, <https://doi.org/10.1175/JAS-D-13-0399.1>.
- Ogden, F. L., 2016: Evidence of equilibrium peak runoff rates in steep tropical terrain on the island of Dominica during Tropical Storm Erika, August 27, 2015. *J. Hydrol.*, **542**, 35–46, <https://doi.org/10.1016/j.jhydrol.2016.08.041>.
- Parish, T. R., D. A. Rahn, and D. Leon, 2016: Research aircraft determination of D-value cross sections. *J. Atmos. Oceanic Technol.*, **33**, 391–396, <https://doi.org/10.1175/JTECH-D-15-0173.1>.
- Pasch, R. J., and A. B. Penny, 2016: Tropical cyclone report: Tropical Storm Erika. National Hurricane Center Rep. AL052015, 26 pp., [http://www.nhc.noaa.gov/data/tcr/AL052015\\_Erika.pdf](http://www.nhc.noaa.gov/data/tcr/AL052015_Erika.pdf).
- Rappaport, E. N., 2014: Fatalities in the United States from Atlantic tropical cyclones: New data and interpretation. *Bull. Amer. Meteor. Soc.*, **95**, 341–346, <https://doi.org/10.1175/BAMS-D-12-00074.1>.
- Raymond, D. J., 1992: Nonlinear balance and potential-vorticity thinking at large Rossby number. *Quart. J. Roy. Meteor. Soc.*, **118**, 987–1015, <https://doi.org/10.1002/qj.49711850708>.
- Reasor, P. D., R. Rogers, and S. Lorsolo, 2013: Environmental flow impacts on tropical cyclone structure diagnosed from airborne Doppler radar composites. *Mon. Wea. Rev.*, **141**, 2949–2969, <https://doi.org/10.1175/MWR-D-12-00334.1>.
- Riemer, M., and M. T. Montgomery, 2011: Simple kinematic models for the environmental interaction of tropical cyclones in vertical wind shear. *Atmos. Chem. Phys.*, **11**, 9395–9414, <https://doi.org/10.5194/acp-11-9395-2011>.
- , —, and M. E. Nicholls, 2010: A new paradigm for intensity modification of tropical cyclones: Thermodynamic impact of vertical wind shear on the inflow layer. *Atmos. Chem. Phys.*, **10**, 3163–3188, <https://doi.org/10.5194/acp-10-3163-2010>.
- Rios-Berrios, R., and R. D. Torn, 2017: Climatological analysis of tropical cyclone intensity changes under moderate vertical wind shear. *Mon. Wea. Rev.*, **145**, 1717–1738, <https://doi.org/10.1175/MWR-D-16-0350.1>.
- Smith, R. B., Q. Jiang, M. G. Fearon, P. Tabary, M. Dorninger, J. D. Doyle, and R. Benoit, 2003: Orographic precipitation and air mass transformation: An Alpine example. *Quart. J. Roy. Meteor. Soc.*, **129**, 433–454, <https://doi.org/10.1256/qj.01.212>.
- , P. Schafer, D. J. Kirshbaum, and E. Regina, 2009a: Orographic precipitation in the tropics: Experiments in Dominica. *J. Atmos. Sci.*, **66**, 1698–1716, <https://doi.org/10.1175/2008JAS2920.1>.
- , —, —, and —, 2009b: Orographic enhancement of precipitation inside Hurricane Dean. *J. Hydrometeorol.*, **10**, 820–831, <https://doi.org/10.1175/2008JHM1057.1>.
- , and Coauthors, 2012: Orographic precipitation in the tropics: The Dominica Experiment. *Bull. Amer. Meteor. Soc.*, **93**, 1567–1579, <https://doi.org/10.1175/BAMS-D-11-00194.1>.
- Susca-Lopata, G., J. Zawislak, E. J. Zipser, and R. F. Rogers, 2015: The role of observed environmental conditions and precipitation evolution in the rapid intensification of Hurricane Earl (2010). *Mon. Wea. Rev.*, **143**, 2207–2223, <https://doi.org/10.1175/MWR-D-14-00283.1>.
- Tang, B., and K. Emanuel, 2012: Sensitivity of tropical cyclone intensity to ventilation in an axisymmetric model. *J. Atmos. Sci.*, **69**, 2394–2413, <https://doi.org/10.1175/JAS-D-11-0232.1>.
- Wu, C.-C., and Y.-H. Kuo, 1999: Typhoons affecting Taiwan: Current understanding and future challenges. *Bull. Amer. Meteor. Soc.*, **80**, 67–80, [https://doi.org/10.1175/1520-0477\(1999\)080%3C0067:TATCUA%3E2.0.CO;2](https://doi.org/10.1175/1520-0477(1999)080%3C0067:TATCUA%3E2.0.CO;2).
- Wu, L., H. Su, R. G. Fovell, T. J. Dunkerton, Z. Wang, and B. H. Kahn, 2015: Impact of environmental moisture on tropical cyclone intensification. *Atmos. Chem. Phys.*, **15**, 14041–14053, <https://doi.org/10.5194/acp-15-14041-2015>.